PNAS
www.pnas.org

Supplementary Information for

Ontogeny of the anuran urostyle and the developmental context of evolutionary novelty

Gayani Senevirathne[1], Stephanie Baumgart[1], Nathaniel Shubin[2], James Hanken[3] & Neil H. Shubin[1]*

Neil H. Shubin

Email: nshubin@uchicago.edu

This PDF file includes:

Supplementary text and Supplementary Table
Figures and Figure legends for S1 to S16
Legends for Datasets S1, S2, S3

Other supplementary materials for this manuscript include the following:

Datasets S1, S2, S3

www.pnas.org/cgi/doi/10.1073/pnas.1917506117

Supplementary Information Text

Detailed description of the axial column development.

Majority of the postcranial skeletal elements complete the ossification prior to the metamorphic climax. To observe developmental timing of the urostyle formation in *Xenopus tropicalis*, we stained cartilage and bone, using alcian blue and alizarin red, respectively. The presacral vertebrae are recognized as I–IX, where the first vertebra is called the atlas, the IX vertebra – is the sacrum. A typical vertebra has two prezygapophyses (at the rostral end), two postzygapophyses (at the caudal end) and two transverse processes. The first presacral, atlas (= cervical vertebra) is distinct in having cervical condyles, which are articulating surfaces with the occipital condyles, and bears only postzygapophyses.

The cartilaginous precursors of the neural arches of presacral I–VI were formed by stage 45 (Fig. S1). By stage 50, VII–IX neural arches also formed. By stage 54, base of the pedicels of the presacrals start to ossify (starting from the part where they are attached to the lateral ends of each centrum); cartilaginous models for each presacral, sacrum and postsacral I (PSI; (contributes to the future urostyle), also form. All the neural arch pedicels of the presacrals and sacrum have ossified by stage 55 (Fig. S1). By stage 58 (before the metamorphic climax), the centra of presacrals and sacrum have fused medially and also with left and right neural arch pedicels corresponding to each vertebra; the PSI centrum is fused medially (Fig. 1A, C). When the metamorphic climax is initiated (stage 59), the neural arch pedicels of the PSI fuse together, forming the anterior-end of the cone-shaped coccyx. PSI is triangular shaped, reduced in width compared to the rest of the vertebrae (Fig. 1A–C). By stage 61, the neural pedicels of the PSII ossify, and subsequently extends in length with development. The hypochord ossification was initiated ventral to the notochord and PSII, as a slender ossifying stripe, ventral to the PSII (Fig. 1A–C). The hypochord extends in length anteriorly and posteriorly (Fig. 1C). By stage 63, transverse processes of presacrals II–VIII, sacrum and PSI, which are connected to the neural arches laterally start to ossify. The PSIII neural arches formed by stage 64, and PSII and PSIII extend in length both anteriorly and posteriorly (Fig. 1C).

Concomitantly, the hypochord also increased in length, and extended up to the anterior-most margin of the sacrum and the posterior-most margin of the PSIII, anteriorly and posteriorly. By stage 65 and 66, the notochord degenerates; PSII and PSIII fuse together and form two strips of ossifications losing the myomere boundaries. PSI fuses with the anterior margins of PSII (Fig. 1C). At the end of metamorphosis, coccyx (cone-shaped) fuses synostically with the hypochord (a cylindrical rod).

A detailed description of osteocyte-chondrocyte differentiation at the sites of urostyle development.

The cells contributing to the coccyx has a mesodermal origin [12], and the ossifying hypochord is thought to have an endodermal origin [16, 18, 19]. To get a clear understanding of how cells differentiate into bone-forming cell types, we conducted histology for sectioned-tissues. The descriptions initially describe the premetamorphic/prometamorphic condition, and then discuss the differentiation patterns during the metamorphic climax.

Coccyx: The somites 9–12 contribute to the coccyx [12, 26]. The sclerotome in frogs is formed and segregated normally in both rostral and caudal somites [26]. Before metamorphosis, sclerotomal mesenchymal cells (MS) are present within the extracellular matrix (ECM) around the spinal cord, dorsal to the notochord (Fig. 2A–B), and sclerotome-derived mesenchymal cells are not observed ventral to the notochord (Fig. S6). The MSs aggregate and form the neural arch condensations for PSI by stage 57; these eventually form immature chondrocytes (IC) (Fig. 2A– A''). By stage 61, osteoblasts form and cover the mature chondrocytes of the PSI, and the neural arches fused medially (Fig. 2C'). MSs condense and form immature and mature chondrocytes, forming the neural arches of PSII (Fig. 2D–D''). Osteoblasts arrange around the anterior-half of the PSII cartilaginous neural arch and secrete bone matrix (Fig. 2C–C''). Cartilaginous matrix of PSII was deposited; perichondrium forms surrounding anterior-half of the PSII cartilaginous condensation. Subsequently, the MSs continue to condensate, extending posteriorly from each neural arch of PSII. By stage 64 PSIII also starts to ossify in a similar manner as PSII. PSII-III neural arches ossify first, then the cartilaginous matrix connecting the arches ossify, forming two longitudinal stripes;

finally, the two strips of ossifications fuse medially (Fig. 2E–E'') and also with the PSI anteriorly. Periosteum forms surrounding the coccyx (Fig. 2E').

Chronological events of how muscles, neurons, and vasculature change

Here, we offer a possible scenario and chronological events as to how the anuran urostyle develop and the order in which the neuromuscular skeleton, vasculature, and innervation change. Close to metamorphic climax: the PSI is formed, and MSs/chondrocytes forming the PSII are also aggregated; myomeres are made of large fibres and are referred to as DT, extends through out body and tail; spinal nerves extend up to the end of tail; DA, PCV, and DAV present. With the onset of metamorphosis, the hypochord ossifies. First thing to change are the muscle fibres: muscles undergo cell proliferation, starting from the most-dorsal and lateral areas (Fig. 6A',B', white arrows indicate newly forming muscles). At the same time, innermost muscles surrounding the notochord and most-ventral muscles (Fig. 6E') undergo apoptosis. Longismuss dorsi (LD) is the first muscle to form, which is connected to the coccyx. The spinal nerves are still intact and extend till the end of the tail; DA, PCV, and DAV present. By stage 63, the hypochord and coccyx has reached their maximum length posteriorly (up to mytome XIV). coccygeoiliacus (CI) starts to form (Fig. 3B), and, at the same time, the primary myomeres within the most lateral and most dorsal areas undergo apoptosis (Fig. 6F,F'). The CS is the last muscle to form, and the ventral-most muscles degenerate completely (Fig. 3F'', Fig. 6G,G',H,H''). With the DA occlusion, the tail regression happens rapidly, and the degenerating tail also loses its neurons. Neuron degeneration is last to happen within the urostyle region, and this concords with previous studies that looked at tail neuron degeneration ([56] Brown, 1946); during metamorphosis, neurons are the slowest to be absorbed ([56] Brown, 1946) (Fig. 4). Finally, when coccyx and hypochord fuses, the spinal cord changes its morphology, and forms the filum terminale (Fig. 4F,F'; Fig. S5), with the loss of tail.

Supplementary Table 1: Details of the antibodies used in the current study.

Antibody	Source	Identifier	Dilution
Anti- Myomesin (mouse monoclonal)	DSHB	mMaC myomesin B4	1:20
Anti- Titin (mouse monoclonal)	DSHB	9D10	1:20
Anti- MyHC (mouse monoclonal)	DSHB	MF20	1:20
Anti- Tropomyosin (mouse monoclonal)	DSHB	CH1	1:20
Anti-Caspase3 (mouse monoclonal)	abcam	Abcam13847	1:1000
Anti-acetylated Tubulin (mouse monoclonal)	Sigma	T7451	1:1000
Anti-Laminin	DSHB	3H11	1:25
Antibody for skeletal muscles	DSHB	12-101	1:50

Fig. S1. Axial skeletal formation in early postembryonic *Xenopus tropicalis*. NF stage 51 lateral (A) and dorsal (B); stage 55 lateral (C) and dorsal (D); stage 58 lateral (E) and dorsal (F). Cartilaginous precursors of the vertebrae form by stage 51; the neural arch ossifies first; centra, prezygapophyses, and postzygapophyses ossify next. Presacral vertebrae I–VIII, the sacrum, and postsacral vertebrae I are formed prior to metamorphosis. Vertebrae are numbered from I to IX. Abbreviations: CN, centrum; PD, pedicel; PRZ, prezygapophyses; PS, postsacral; PSZ, postzygapophyses; SA, sacrum.

Fig. S2. Whole-mount in-situ hybridization and transverse cross-sections for *Pax9* at stage 27, showing that sclerotome-derived cells are around the spinal cord, across somites I–XIII. (A) Whole-mount in-situ hybridization embryo at stage 27. *Pax9* expression is seen in somites, anterior-to-posterior. Transverse cross sections across (B) somite III, (C) somite IV, (D) somite V, (E) somite VIII, and (F) somite XI.

Fig. S3. Haematoxylin- and eosin-stained transverse histological sections and CT scans of *Xenopus tropicalis*, highlighting hypochord ossification as a midline structure, ventral to the notochord. Cross-sections across a presacral vertebra (A, D, G, J); across the sacrum-urostyle junction (B, E, H, K); and across a posterior part of the notochord (C, F, I, L). Histological sections depict the highlighted portions of the CT orthoslices. Abbreviations: CX, coccyx; DA, dorsal aorta; DLV, dorsal lateral anastomosing vein; NT, notochord; PCV, posterior cardinal vein; PD, pedicel; SC, spinal cord.

Fig. S4. Hall-Brunt Quadruple (HBQ) stained sagittal sections highlighting cartilage (blue) and bone (red), focusing on the ossifying hypochord at stages 59 (A, A’), 60 (B, B’), 63 (C, C’) and 64 (D, D’). Hypochordal ossification is initiated ventral to the notochord and dorsal to dorsal aorta. Notochord degenerates with the fusion of coccyx and hypochord. Abbreviations: DA, dorsal aorta; HY, hypochord; NS, notochordal sheath; NT, notochord; PS, postsacral vertebra.

Fig. S5: HBQ-stained transverse cross sections, at stage 60, depicting the development of the hypochord. Cells aggregate ventral to the notochord and dorsal to the dorsal aorta (A, A', B, B'). No hypochordal cells are present in the tail region (C, C'). Abbreviations: DA, dorsal aorta; HY, hypochord; PCV, posterior cardinal vein; NT, notochord.

Fig. S6. A transverse cross-section across trunk myotome XII at stage 61, highlighting migrating cells during hypochord formation. White arrows point at the migrating cells with filopodia.

Fig. S7. Bone- and cartilage-stained tadpoles, focusing on the posterolateral rotation of the pelvic girdle. Red stars demarcate the acetabulum. (A) stage 58, (B) stage 61, (C) stage 64, and (D) stage 66.

Fig. S8. Methimazole-treated stage-54 tadpoles (A, B, C), in which thyroid hormone production was prevented. The axial column ossifies, including the rudimentary neural arches of vertebrae X and XI, but formation of the hypochord is disrupted even after two months. Control tadpoles metamorphosed and had a urostyle (D).

Fig. S9. Coronal sections of the spinal cord, before (A) and after (B) metamorphosis. Sagittal section (C) and transverse sections (D, E) of a stage 59, *Xenopus tropicalis* tail. Phalloidin (green) stains the extracellular matrix, DAPI (blue) stains nuclei, and tubulin (red) stains nerves.

Fig. S10. Transverse cross-sections across trunk myotome XII at stage 61, beginning of metamorphic climax (A–C). Phalloidin (green) stains the extracellular matrix, DAPI (blue) stains nuclei, and laminin (B) (red) stains muscle fibers. (C) Illustration of the stage 61 transverse cross section. DT, dorsalis trunci.

Fig. S11. Dorsal views of whole-mount immuno-stained specimens for muscles using 12-101 antibody (A) and neurons using acetylated tubulin (B), at stage 65.

Fig. S12. Sagittal cross sections across the developing urostyle to observe the sarcomere protein organization before metamorphosis (A, D, G), during metamorphic climax (B, E, H), and end of metamorphosis (C, F, I). Before metamorphosis, sarcomere proteins are distinguishable with a banded pattern; during metamorphosis the banded pattern of the sarcomeres become disorganized; and after metamorphosis the banded pattern re-appear.

A, B, C are bright-field photographs; titin is shown in red; myomesin in yellow, and tropomyosin in green

Fig. S13. Transverse cross-sections across the urostyle, depicting skeletal muscle fibers (stained using an antibody for myosin) at stages 57 (A, A'), 61 (B, B'), and 65 (C, C') Myosin is shown in red and DAPI (nuclei) in blue. Abbreviations: DA, dorsal aorta; HY, hypochord; NT, notochord; SC, spinal cord.

Fig. S14. Transverse cross-sections of the CT-scanned tadpoles at stage 59 (A–D and A'–D'). The developing hypochord is shown in yellow; the dorsal aorta (DA) in red, and the posterior cardinal vein (PCV) in blue. With ossification of the hypochord between the notochord and DA the diameter of the DA is reduced, causing an occlusion at the posterior-most end of the hypochord (stage 64, E–H and E'–H').

Fig. S15. Transverse cross-sections of the CT-scanned tadpoles at stage 66 (A–C and A'–C'). The dorsal aorta is red, hypochord in yellow, and renal vein in blue.

Fig. S16. Cell death (A, B, E, F) and cell proliferation (C, D, G, H) during premetamorphic stages. Both processes are concentrated along the endoderm and the tadpole skin.

Dataset. S1 (separate file, open using Adobe Reader to access the 3D view). CT-scanned tadpole, highlighting the major blood vessels, stage 59 (prometamorphosis).

Dataset. S2 (separate file, open using Adobe Reader to access the 3D view). CT-scanned tadpole, highlighting the major blood vessels, stage 63 (metamorphic climax).

Dataset. S3 (separate file, open using Adobe Reader to access the 3D view). CT-scanned tadpole, highlighting the major blood vessels, stage 66 (metamorphic climax).

SUPPLEMENTARTY MATERIAL

Supplementary Figure 1

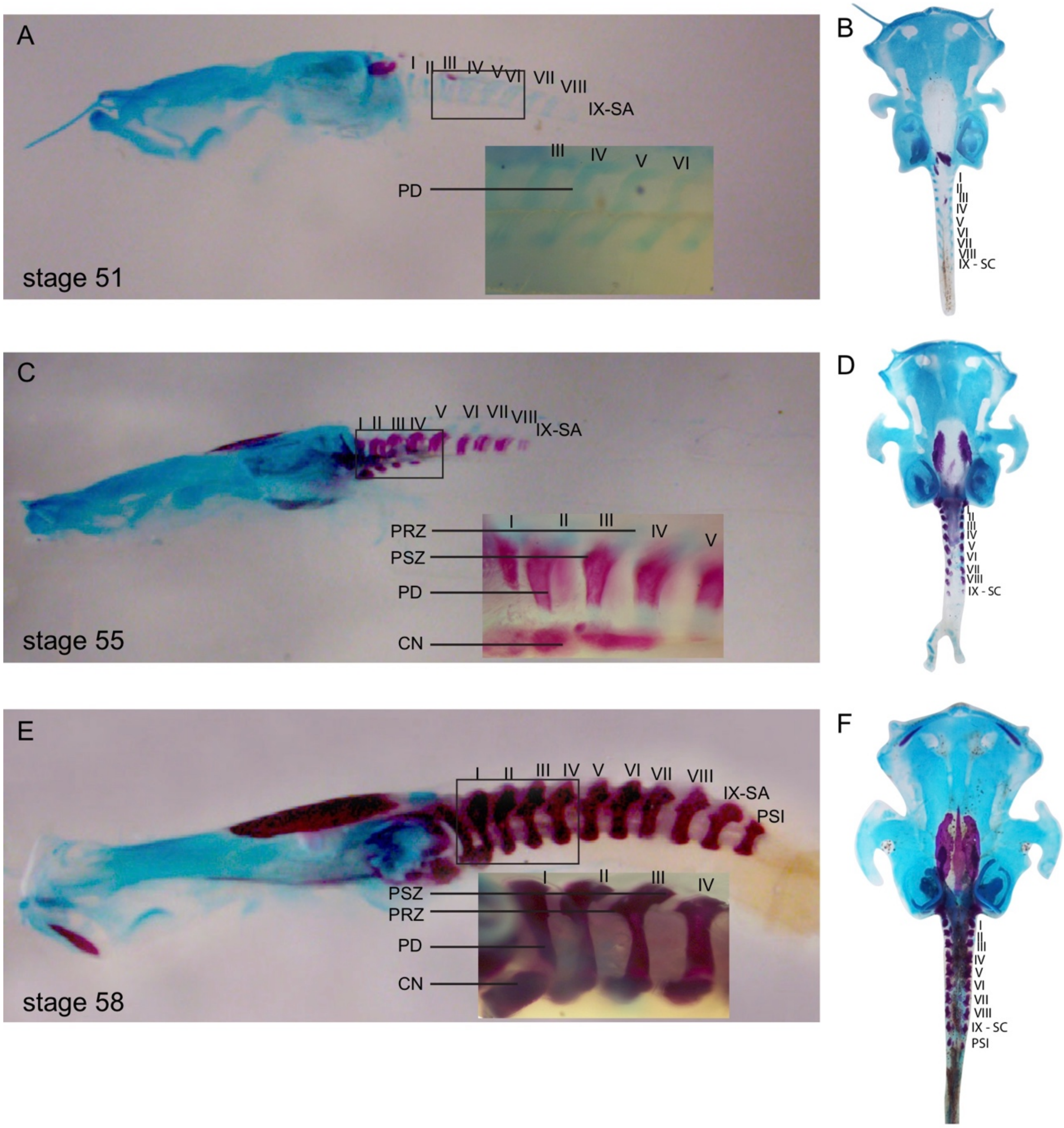

Supplementary Figure 2

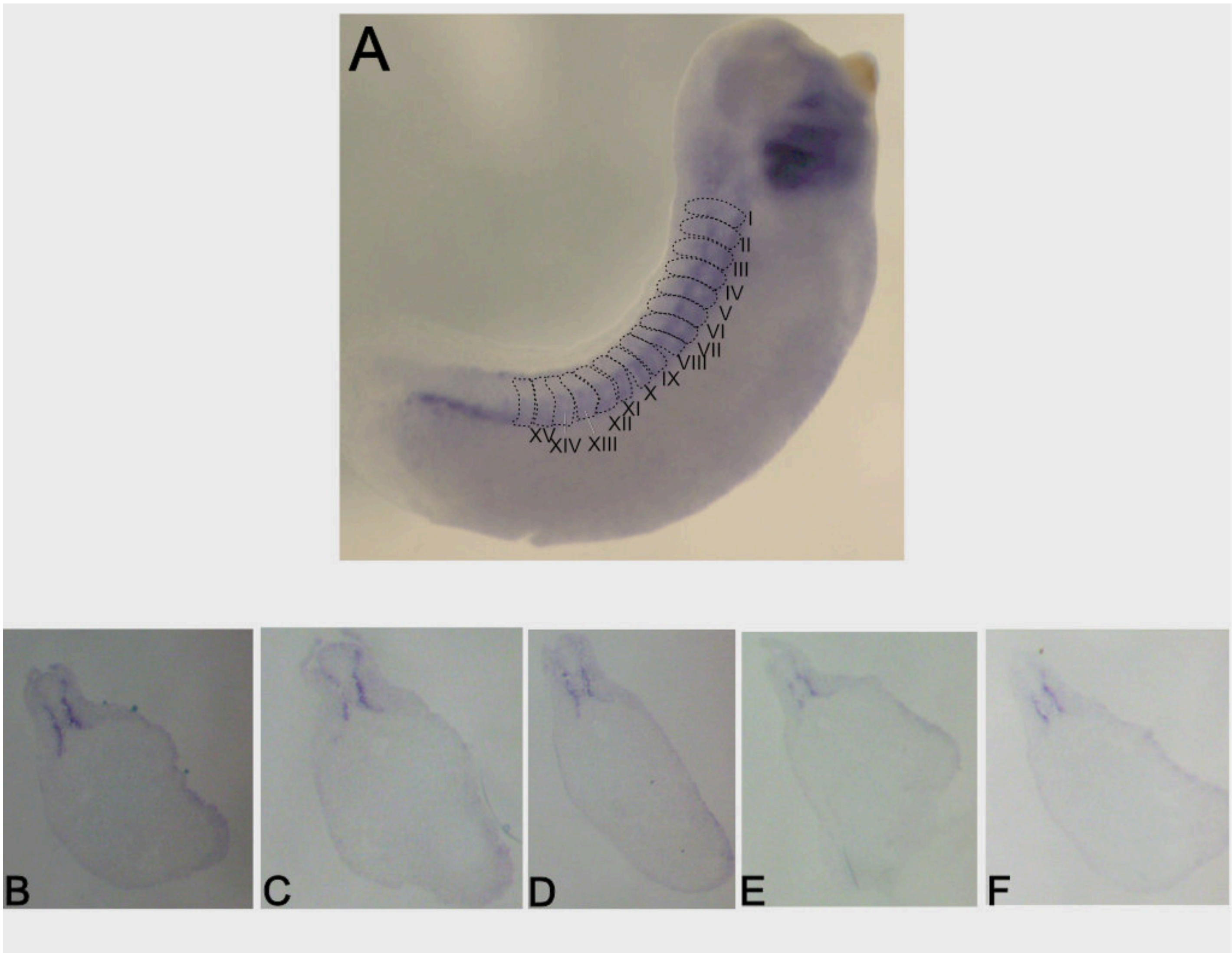

Supplementary Figure 3

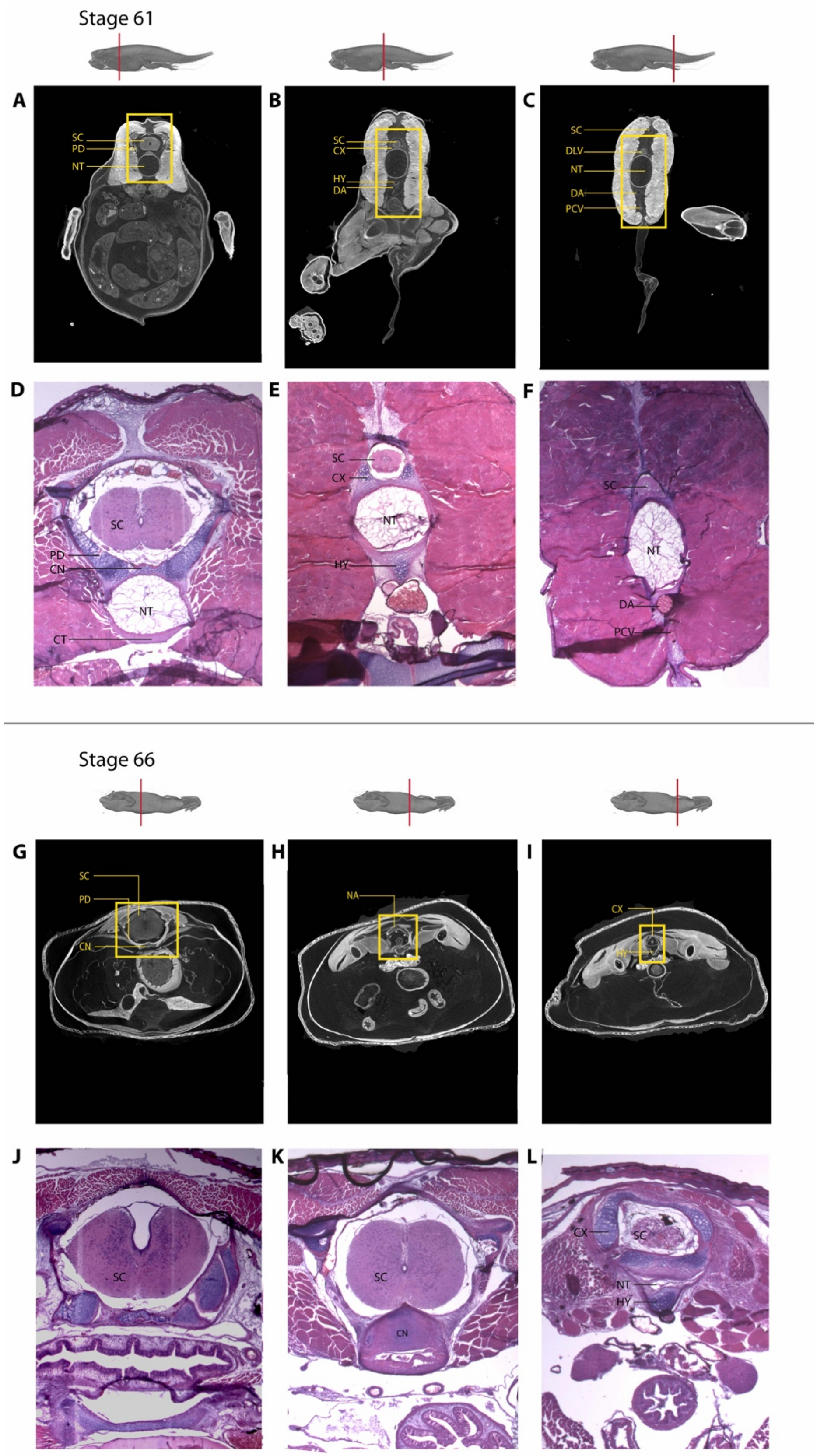

Supplementary Figure 4

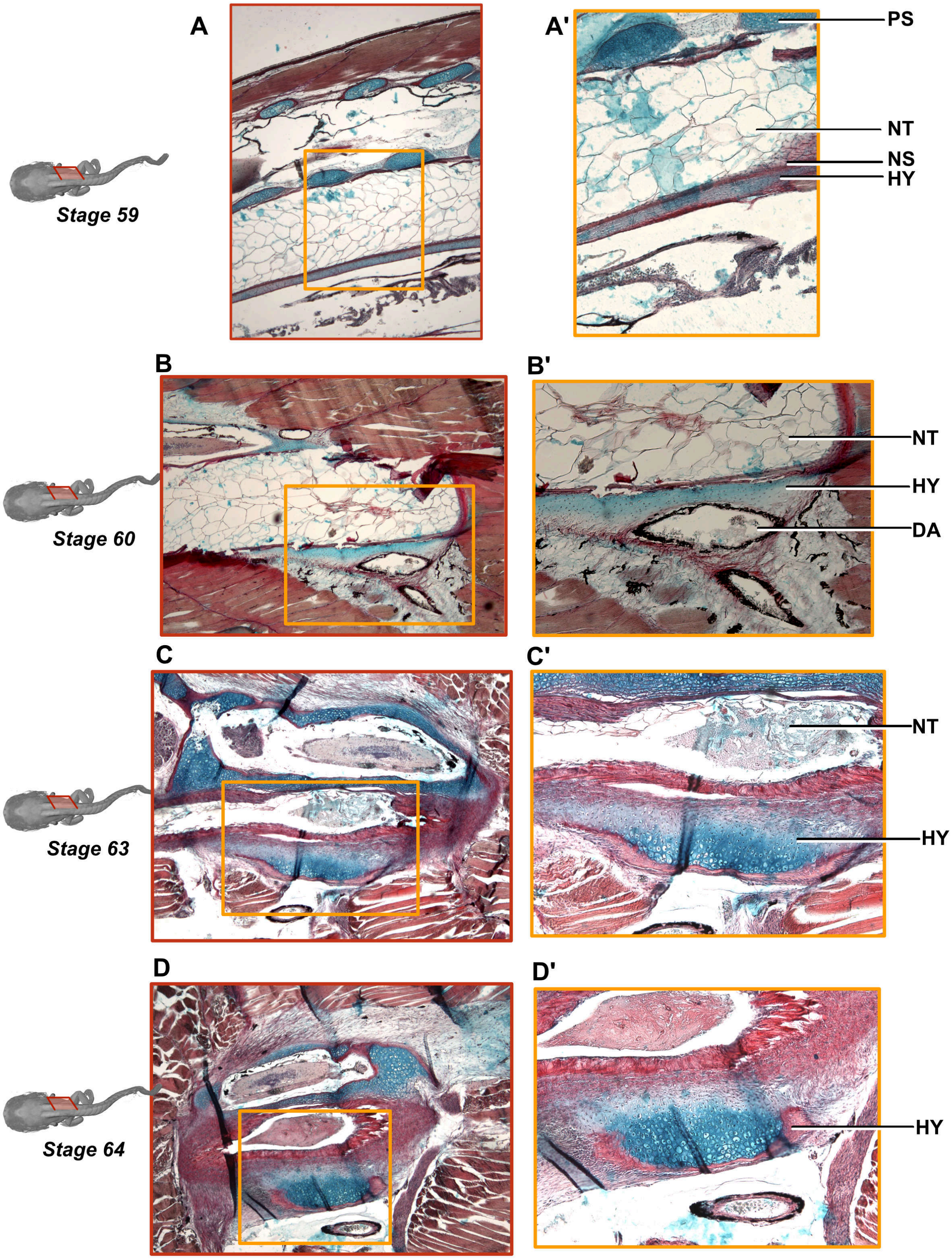

Supplementary Figure 5

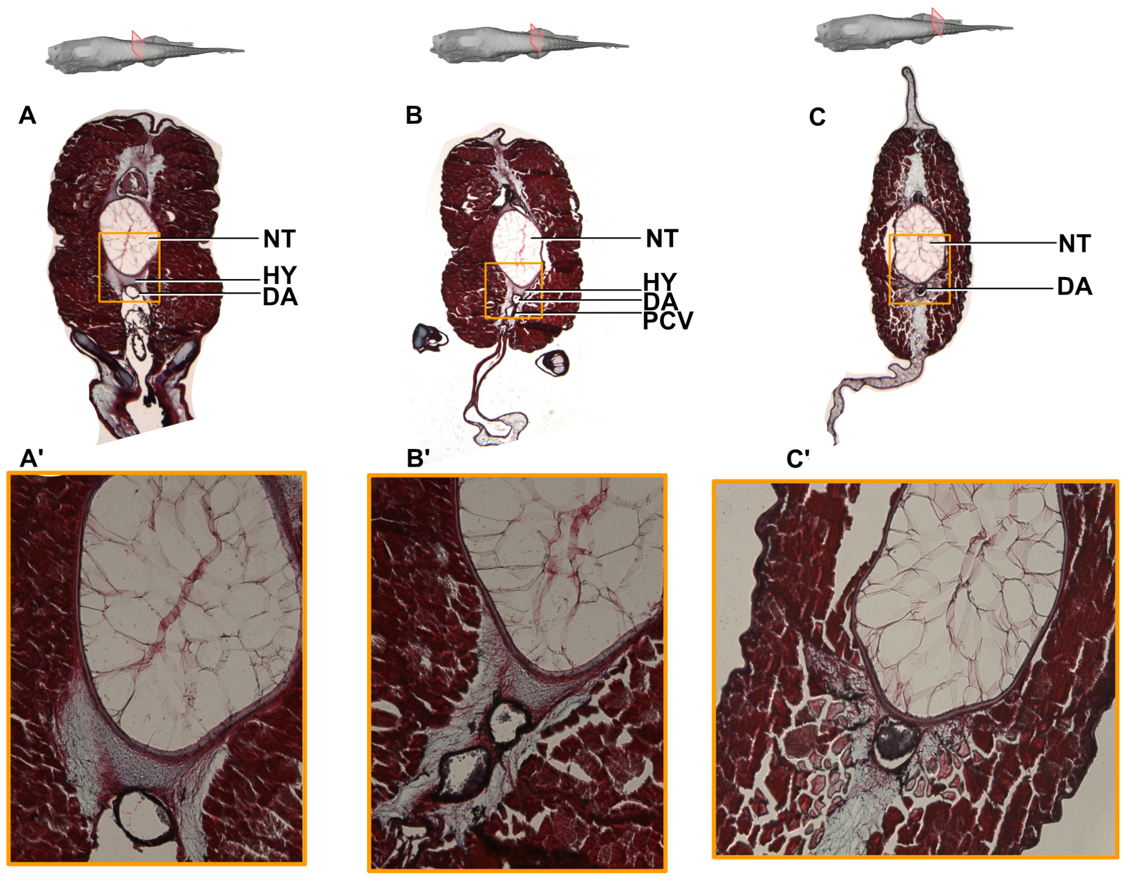

Supplementary Figure 6

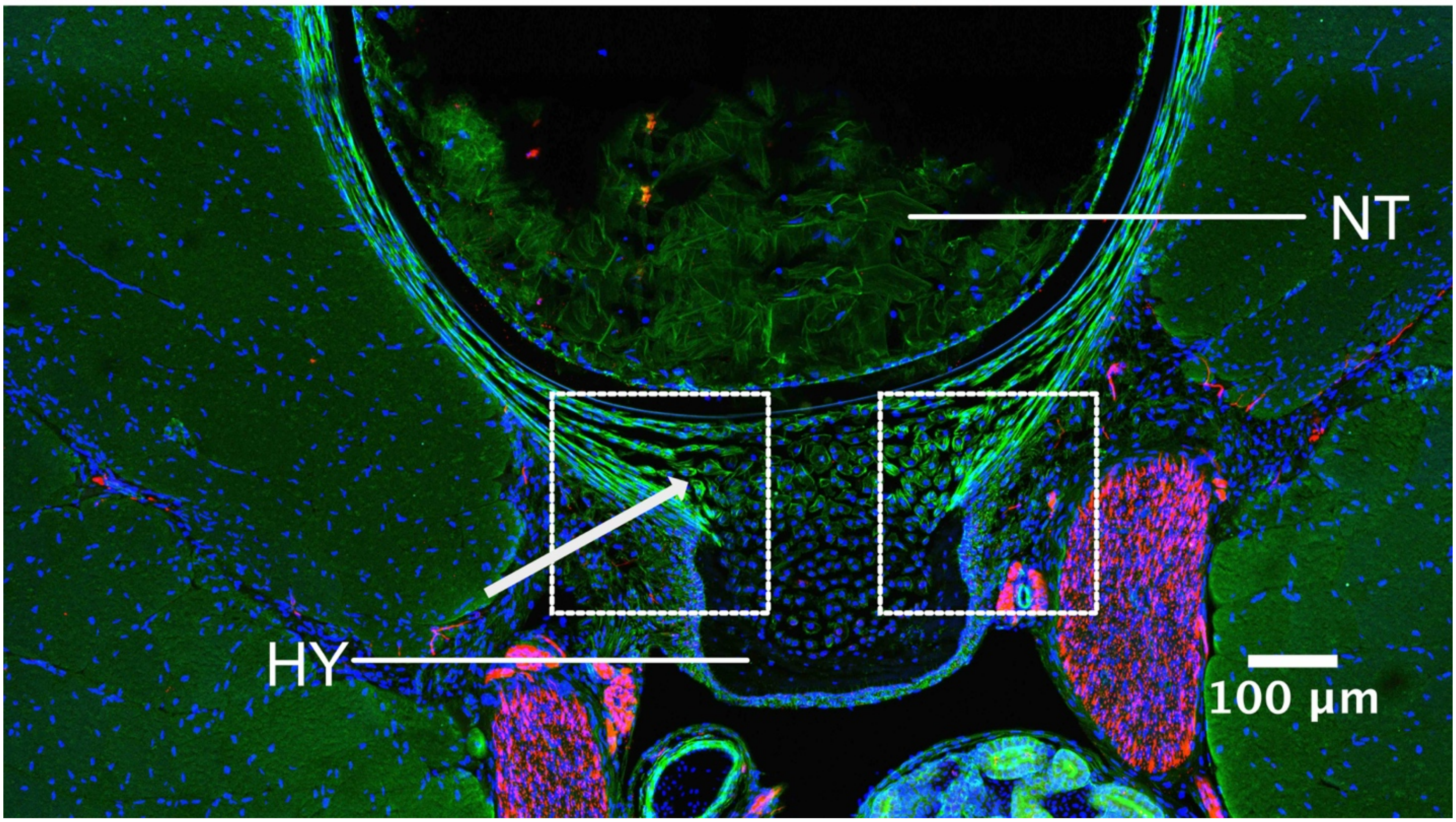

Supplementary Figure 7

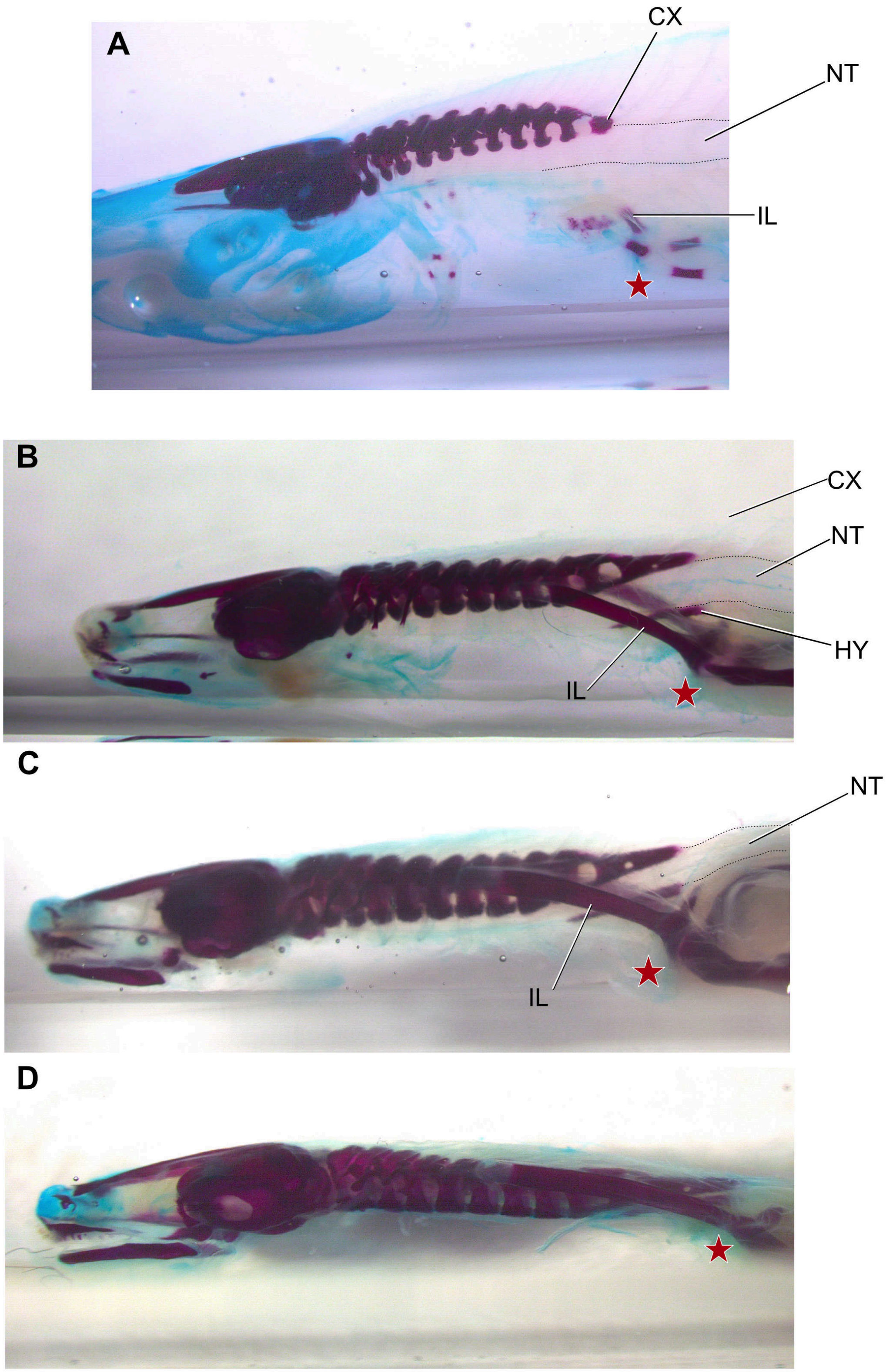

Supplementary Figure 8

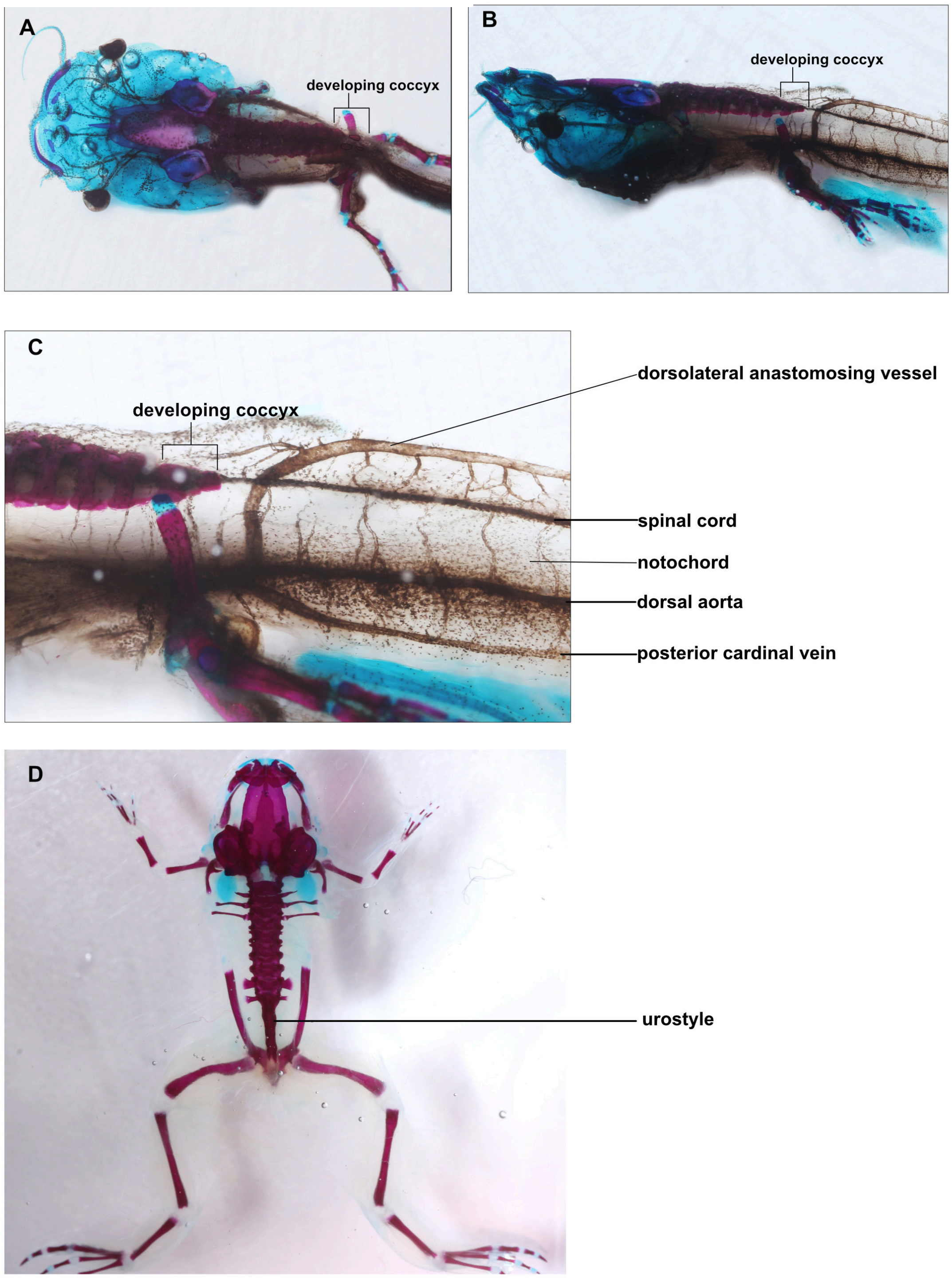

Supplementary Figure 9

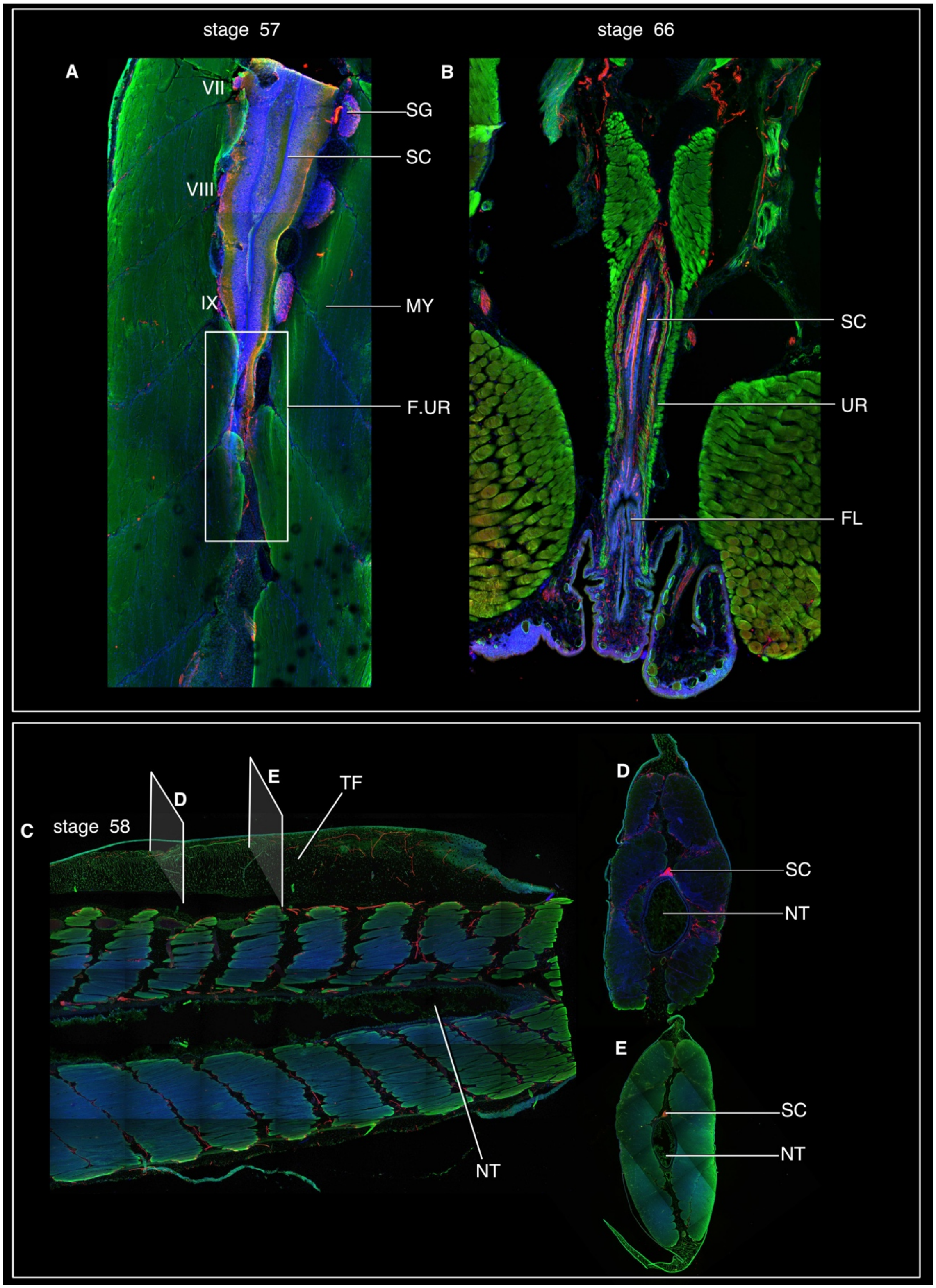

Supplementary Figure 10

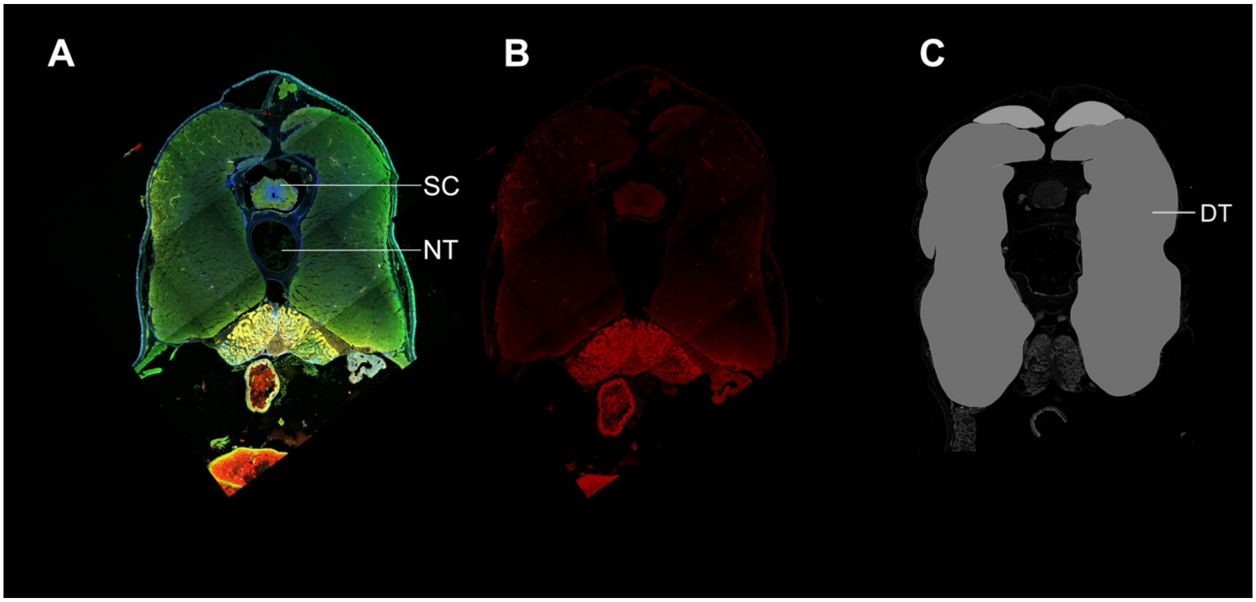

Supplementary Figure 11

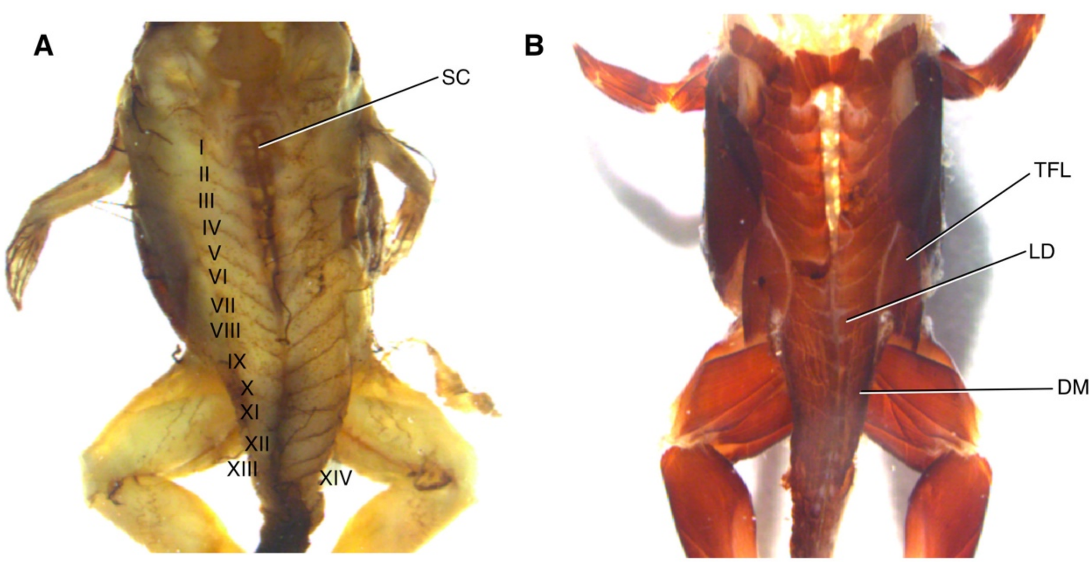

Supplementary Figure 12

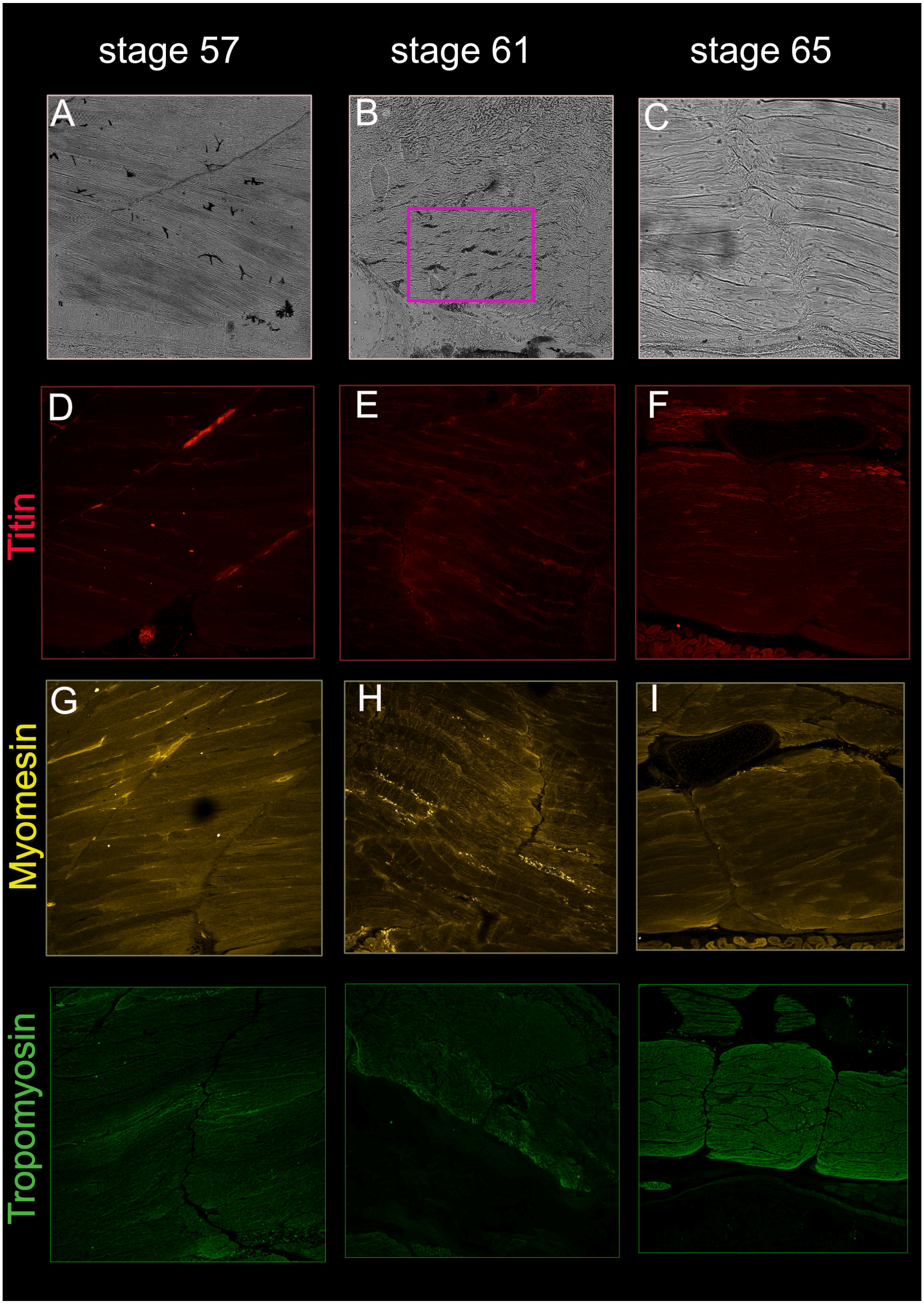

Supplementary Figure 13

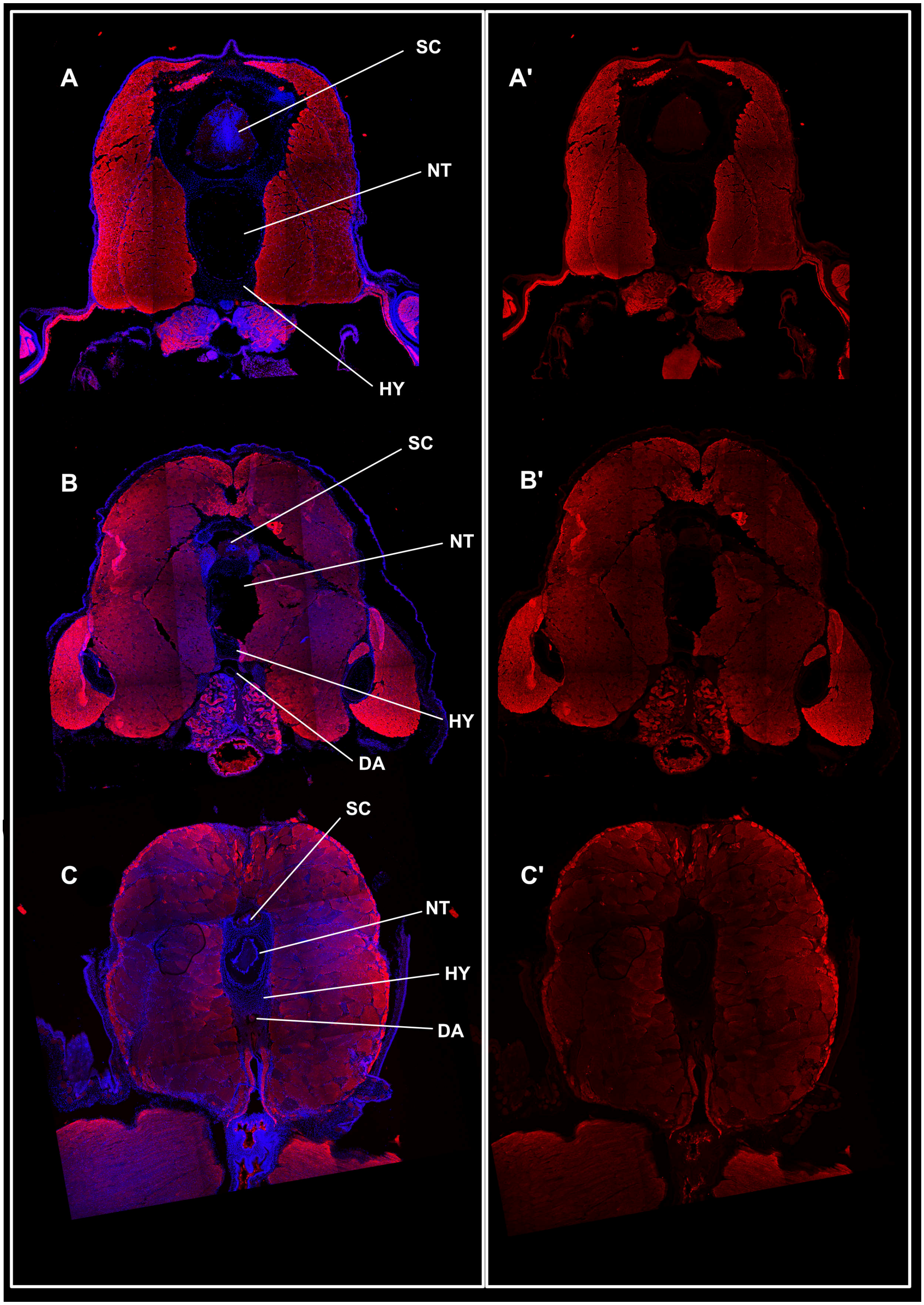

Supplementary Figure 14

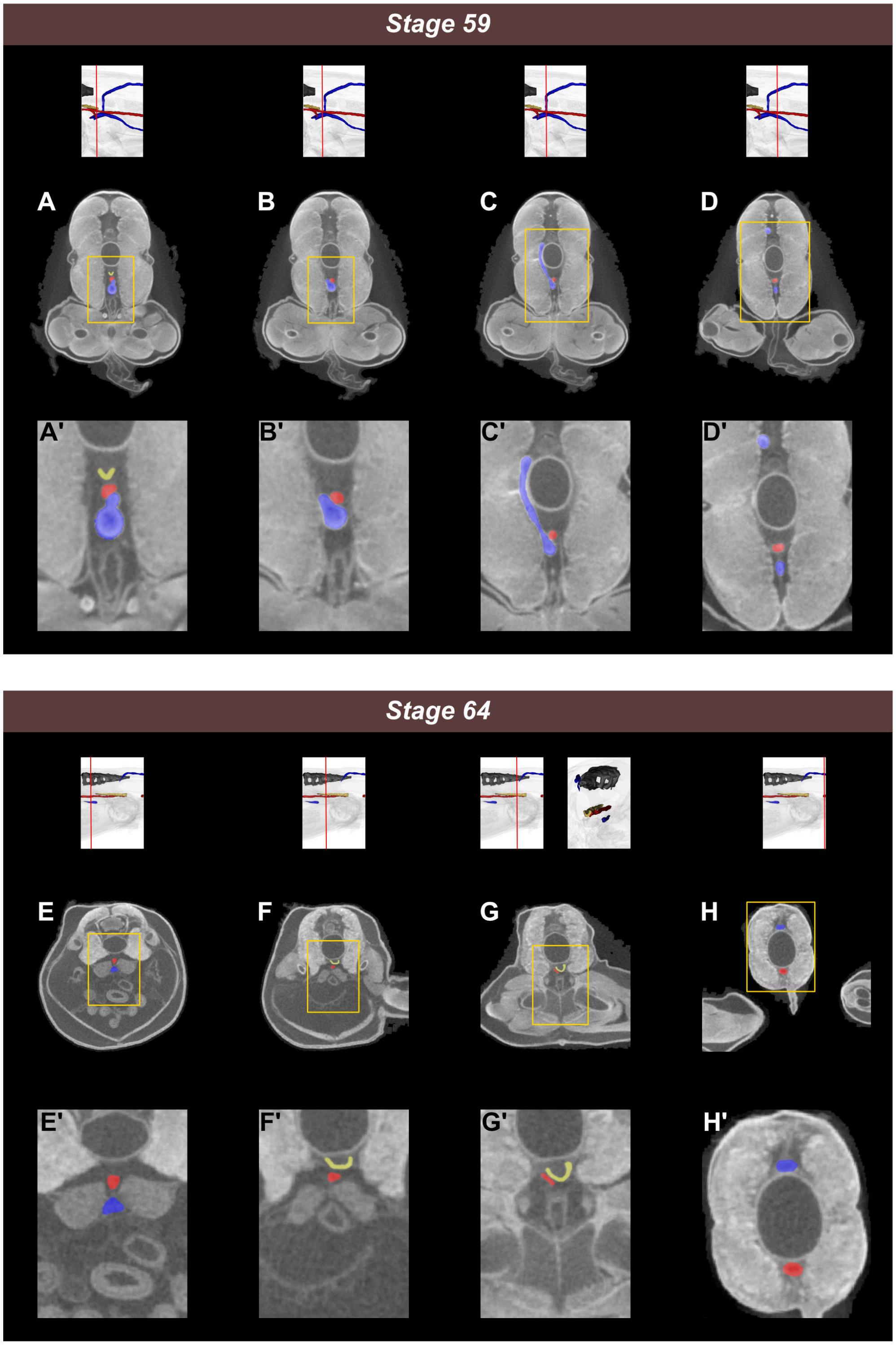

Supplementary Figure 15

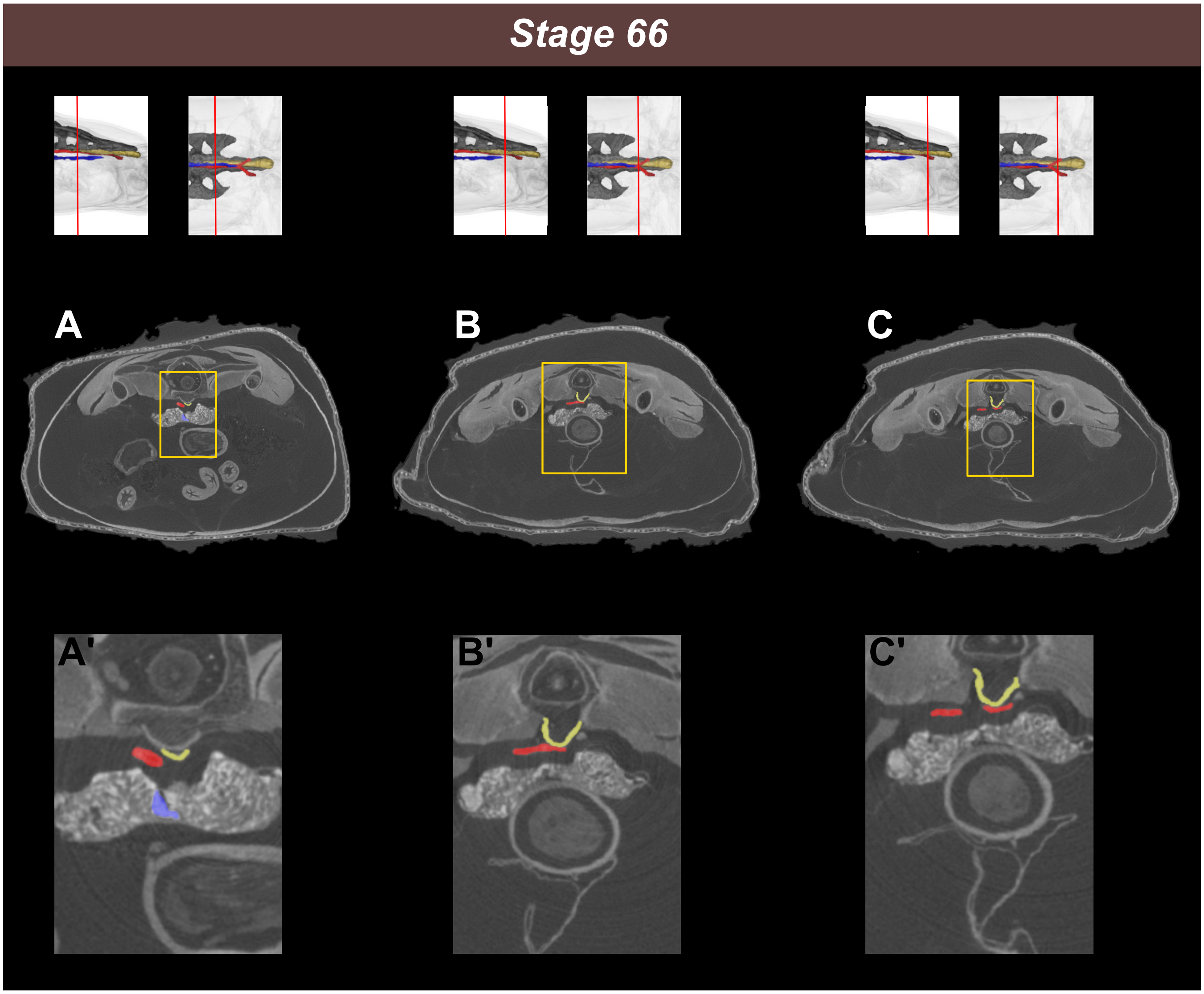

Supplementary Figure 16